higher emissivity values (0.8–0.9) on the plains and on the other crater floors and to investigate whether young lava flows also exhibit low emissivities. (This work was conducted at the Jet Propulsion Laboratory, California Institute of Technology, under contract with the National Aeronautics and Space Administration.)

References: [1] Schaber et al. (1992) *JGR*, in press. [2] Klose et al. (1992) *JGR*, in press. [3] Pettengill et al. (1991) *Science, 252*, 260–265. [4] Campbell et al. (1992) *JGR*, in press. [5] Olhoeft G. R. and Strangway D. W. (1975) *EPSL, 24*, 394–404. [6] Tyler et al. (1976) *Science, 193*, 812–815. [7] Campbell M. J. and Ulrichs J. (1969) *JGR, 74*, 5867–5881. [8] Pettengill et al. (1988) *JGR, 93*, 14881–14892.

N93-14393

FLOOR-FRACTURED CRATER MODELS FOR IGNEOUS CRATER MODIFICATION ON VENUS.

R. W. Wichman and P. H. Schultz, Department of Geological Sciences, Brown University, Providence RI 02912, USA.

Introduction: Although crater modification on the Earth, Moon, and Mars results from surface erosion and crater infilling, a significant number of craters on the Moon also exhibit distinctive patterns of crater-centered fracturing and volcanism that can be modeled as the result of igneous crater modification [1–5]. Here, we consider the possible effects of Venus surface conditions on this model, describe two examples of such crater modification, and then briefly discuss the constraints these craters may place on conditions at depth.

Floor-fractured Crater Model: On the Moon, most floor-fractured craters occur near the lunar maria [1,6,7] or along basin ring faults [5], and commonly contain ponded mare units and dark mantling deposits [1,8,9]. Fracturing is confined to the crater interior, and, in the more modified craters, uplift of the crater floor as a single coherent unit results in a distinctive moatlike failure zone in the crater wall region [1,4]. In some cases, later volcanism floods this moat structure or buries the entire floor [1,3].

Although viscous relaxation can produce uplift of the crater floor [10–12], shallow, laccolithlike intrusion beneath the crater floor provides a model consistent with observations on the Moon. As discussed elsewhere [1,4,5], intrusions apparently begin in a neutral buoyancy zone near the base of the crater-centered breccia lens through the lateral growth of a sill-like magma body. Both the increased lithostatic pressures and diminished impact brecciation beneath the crater walls, however, enhance resistance to such lateral intrusion growth beyond the crater floor region, thereby evolving into vertical, laccolithic intrusion growth described by [13]. During vertical growth, the crater floor rises through a pistonlike uplift, while ring faulting near the edge of the intrusion produces the moat structures outside this uplift.

For a laccolithic intrusion, crater modification is controlled by parameters that allow assessing conditions at depth [4,5]. Since elastic deformation should not thin the uplifted crater floor section, the amount of floor uplift essentially reflects the intrusion thickness. If the uplifted floor diameter delineates the laccolith size at depth, then the model [13] can be used to estimate both the magma pressure driving deformation and an effective thickness for the crater floor materials overlying the intrusion. The derived magma pressures then help constrain the length of the magma column beneath the intrusion, whereas the inferred floor thickness provides a model for both the intrusion depth and breccia thickness in a given crater [4,5].

Floor-fractured Craters on Venus: The evidence for widespread volcanism on Venus [14] would seem to favor igneous crater modification. Four significant differences between conditions on Venus and on the Moon may modify the processes of crater-centered igneous intrusion. First, where the anorthositic crust on the Moon is apparently equivalent in density or less dense than most mare magmas [15], the basaltic crust on Venus should be denser than basaltic melts and may be thinner than the lunar crust as well. Consequently, basalt magmas on Venus are more likely to rise to the surface than magmas on the Moon, perhaps decreasing the likelihood of crater-centered intrusions at depth [4]. Second, the lunar crust has been extensively fractured by successive, overlapping impact events. The resulting combination of a megaregolith and basin ring faults, therefore, provides a number of conduits through which magma can enter individual crater-centered breccias. In contrast, the crust on Venus appears to be more coherent; hence, magma may not favor breccias beneath craters on Venus. Instead, a crater-centered intrusion may first require deformation by a regional fracture system. Third, the higher surface gravity on Venus should reduce the fracture porosity of an impact breccia, thereby reducing the density contrast required for a shallow zone of crater-centered neutral buoyancy. High surface gravity also should consolidate impact breccias at depth, which may produce thinner breccia lenses on Venus than on the Moon. As a result, the uplifted floor plate on Venus should be thinner than on the Moon, and floor fracturing would then be expected to be more polygonal, i.e., reflecting inhomogeneities in the floor rather than acting as a coherent block. Fourth, since the increased surface temperatures on Venus may allow annealing of impact breccias over time, both the fracture density beneath a Venus crater and the probability of an igneous intrusion also may decrease as a function of crater age.

Most impact craters on Venus do not exhibit floor fractures comparable to examples on the Moon. Instead, either volcanic infilling occurs or craters are simply engulfed rather than participate in surface volcanism. Figures 1 and 2, however, illustrate two craters that closely resemble floor-fractured craters on the Moon. For reference, both craters occur in ridged lowland plains with elevations of approximately –500 m to 500 m, relative to the mean planetary radius. The first of these craters (Fig. 1) is 48 km in diameter and exhibits a scarp-bounded central floor plate 32 km in diameter in which an additional pattern of concentric failure can be

Fig. 1. Modified crater centered at 52°S, 196°E. Note the wide outer moat structure surrounding the central floor and the bright scarp along the southwest edge of the central floor plate. Scale bar is ~17 km (enlarged section of C1-45S202;1).

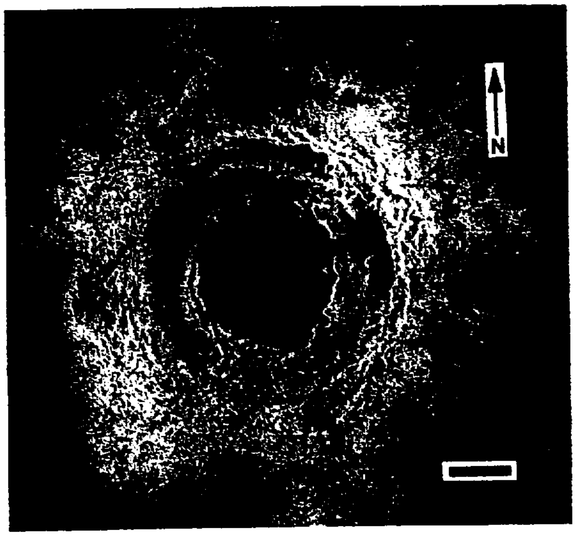

Fig. 2. Mona Lisa Crater, centered at 25.6°N, 25.2°E near the edge of Eisila Regio. Note partial flooding of outer moat structure and bright fracture pattern in the central floor plate. Scale bar is ~17 km (enlarged section of C1-30N027;1).

recognized. Although transected by a number of later wrinkle ridges, both the outer moat region and the central floor appear to be relatively smooth and may reflect a sequence of crater-centered volcanism after the uplift event, also observed in the lunar crater Posidonius. The second crater (Fig. 2) is larger (~75 km diameter) and somewhat less modified. In this case, a bright ridge nearly surrounds the central floor plate, and volcanism has only flooded the central floor and the northern half of the outer moat structure, allowing identification of the moat fractures in the south. Inside the central floor plate, concentric fractures bound the central floor with a set of radial/polygonal fractures in the center of the floor plate. Both craters occur in ridged lowland plains with elevations close to the mean planetary radius. Since the ejecta pattern and the scalloped southern crater rim indicate an oblique impact from the north [16,17], the northward offset of these central fracture patterns relative to the crater center is consistent with the uprange offset of both central peaks and basin rings in other oblique impact structures [5,16,17], whereas the distribution of moat-filling volcanism is consistent with the enhanced failure uprange proposed by [5,18,19] for cavity collapse in an oblique impact event.

The intrusion parameters derived from the relations of [13] can be related to the local crustal structure. For floor uplift of ~1.5 km (inferred for the craters described above), both craters indicate a magmatic driving pressure of ~375 bar for a basaltic melt. If this pressure then reflects the magmastatic head resulting from the density contrast between a basaltic magma (~2800 kg/m^3) and a basaltic crust (3000 kg/m^3), a magma column length of 22 km is indicated for both regions. Since the effective thickness of the floor plate is estimated at 2–6 km for crater 1 and 4–8 km for crater 2, this simple model requires a crustal (basaltic) thickness exceeding ~2530 km. Alternatively, if the basaltic crust on Venus is less than 10–20 km, as proposed in [20], the base of the magma column occurs within a denser mantle unit at depths of less than 20–25 km. If the base of the magma column corresponds to a deep, regional magma chamber, these magma column models should indicate either the base of the basaltic crust or rheological boundaries with the crust or lithosphere [21]. Consequently, the implications of floor-fractured craters on Venus for subsurface density provide an additional test for models of regional crustal structure.

References: [1] Schultz P. H. (1976) *Moon, 15,* 241–273. [2] Schultz P. H. (1978) *GRL, 5,* 457–460. [3] Schultz P. H. (1976) *Moon Morphology.* [4] Wichman R. W. and Schultz P. H. (1991) *LPSC XXII,* 1501–1502. [5] Wichman R. W. (1992) Ph.D. thesis, Brown University. [6] Brennan W. J. (1975) *Moon, 12,* 449–461. [7] Whitford-Stark J. L. (1974) *Nature, 248,* 573–575. [8] Young R. A. (1972) *Apollo 16 Prelim. Sci. Rep.,* NASA SP-315, 29–89 to 29–90. [9] Bryan W. B. et al. (1975) *Proc. LSC 6th,* 2563–2570. [10] Danes Z. F. (1965) *Astrogeol. Stud. Ann. Prog. Rep. A (1964–1965),* 81–100. [11] Scott R. F. (1967) *Icarus, 7,* 139–148. [12] Hall J. L. et al. (1981) *JGR, 86,* 9537–9552. [13] Pollard D. P. and Johnson A. M. (1973) *Tectonophysics, 18,* 261–309. [14] Head J. W. et al. (1992) *Magellan 6 Month Rep.,* in press. [15] Solomon S. C. (1975) *Proc. LSC 6th,* 1021–1042. [16] Schultz P. H. and Gault D. E. (1991) *LPSC XXIII,* 1231–1232. [17] Schultz P. H. (1992) *Magellan 6 Month Rep.,* in press. [18] Wichman R. W. and Schultz P. H. (1992) *LPSC XXIII,* 1521–1523. [19] Schultz P. H., this volume. [20] Grimm R. E. and Solomon S. C. (1988) *JGR, 93,* 11911–11929. [21] Head J. W. and Wilson L. (1992) *JGR, 97,* 3877–3903.

N93-14394

VENUS: GEOCHEMICAL CONCLUSIONS FROM THE MAGELLAN DATA. J. A. Wood, Harvard-Smithsonian Center for Astrophysics, Cambridge MA 02138, USA.

Though the Magellan mission was not designed to collect geochemical or petrological information, it has done so nonetheless. Since the time of the Pioneer Venus mission it has been known that high-altitude (>2.5–5 km) mountainous areas on Venus exhibit anomalously low radiothermal emissivity ($e < 0.6$) [1]. Magellan has greatly refined and extended these observations. The low emissivity requires surface material in the uplands to have a mineralogical composition that gives it a high bulk dielectric constant, >~20. The dielectric constant of dry terrestrial volcanic rocks seldom exceeds 7. The high-dielectric character of high-altitude surface material cannot be a primary property of the local volcanic rock, because there is no reason why rock having the required special mineralogy would erupt only at high altitudes. Therefore it is a secondary property; the primary Venus rock has reacted with the atmosphere to form a mineralogically different surface layer, and the secondary minerals formed are controlled by the ambient temperature, which decreases with altitude on Venus.

Klose et al. [2] showed that, for a plausible assumption of oxygen fugacity in the Venus atmosphere (~10^{-21} bar), variation of the equilibrium weathered mineral assemblage with altitude and temperature would create such a situation: above a few kilometers altitude the stable assemblage includes pyrite (FeS_2) in sufficient abundance to create a "loaded dielectric" with a bulk dielectric constant >~20; at lower altitudes the stable Fe mineral is magnetite (Fe_3O_4), and this is present in insufficient abundance to give rise to such a high bulk dielectric constant. Pettengill et al. [3] first concluded that pyrite was the mineral responsible for the high-dielectric materials observed at high altitudes on Venus.

Fegley et al. [4] reject this interpretation. They note that the gas species COS is much less abundant in the Venus atmosphere than the equilibrium concentration, and argue that the reaction

$$3FeS_2 + 2CO + 4CO_2 = 6COS + Fe_3O_4$$